Cabezas-Rabadán, C.; Pardo Pascual, JE.; Palomar-Vázquez, J.; Fernández-Sarría, A. (2019). Characterizing beach changes using high-frequency Sentinel-2 derived shorelines on the Valencian coast (Spanish Mediterranean). The Science of The Total Environment. 691:216-231. https://doi.org/10.1016/j.scitotenv.2019.07.084

Characterizing beach changes using high-frequency Sentinel-2 derived shorelines on the Valencian coast (Spanish Mediterranean)

Abstract

Shoreline position can be efficiently extracted with subpixel accuracy from mid-resolution satellite imagery using tools as SHOREX. However, it is necessary to develop procedures for deriving descriptors of the beach morphology and its changes in order to become truly useful data for characterizing the coastal dynamism.

A new approach is proposed based on a spatiotemporal model of the beach widths. Divided into 80 m analysis segments, it offers a robust and detailed characterization of the beach state along large micro-tidal regions, with continuous information through time and space. Geographical and temporal differences can be recognized and measured, making it possible to study the beach response both to general factors (as wave conditions) and to punctual anthropic actions (as small sand nourishments).

Widths were defined throughout two and a half years from 60 shorelines (3.04 m RMSE) covering 50 km of the Gulf of Valencia. Important width contrasts appeared along the study site associated with sediment imbalances motivated by sediment traps and other anthropic actions. Segments too narrow for maintaining the recreational function were located and mapped (16% narrower than 30 m). Short-term width changes appeared linked to storm events, with fast retreatments and slow recoveries. Punctually, even small-magnitude nourishments created perceptible changes in width (12,830 m^3 were associated with a 4 m increase).

This novel description of the beach state and its changes from Satellite-Derived Shorelines is useful for coastal management, especially considering the global coverage of these free satellite images.

It may improve the comprehension of coastal processes as well as monitor human interventions on the coast, helping in the decision-making.

Keywords: shoreline-position variability, short-term beach changes, remote sensing, coastal erosion, environmental monitoring, beach nourishment

1. INTRODUCTION

Coastal areas are essential for humans, as they hold important and diverse productive habitats for their settlement, subsistence and development (Schlacher et al., 2008). Therefore, the monitoring of coastal dynamics is critical for the society and economy of these areas. The availability of information is necessary for both scientists and managers in order to understand its functioning and to plan human settlements. In this sense, the analysis of shoreline changes and its evolutionary patterns appears as an essential issue (Boak & Turner, 2005).

Coastal erosion is a global problem (Bird, 1996) that in Europe affects up to 20% of the coasts (EUROSION study, European Commission, 2004). Erosive processes and coastal flooding are expected to increase associated with climate change and sea level rise (Schlacher et al., 2008; IPCC, 2014). Erosion, coupled with the presence of landward barriers of human origin will reduce space for natural life (Nordstrom, 2004; Feagin, 2005) causing important ecosystem loss along the coast. With regard to a recreational function that beaches offer to human beings, erosion will negatively affect the economic exploitation of the beaches and tourism revenues (Alexandrakis et al., 2015). In order to maintain them, monitoring the beach morphology and their physical characteristics will become increasingly necessary (Jiménez et al., 2011; Ballesteros et al., 2018). The beach loss will force coastal managers to response both in the short term (e.g. to occasional episodes of storms) and in the long term to the progressive sea level rise scenarios. As an example, planned retreatment and sacrifice areas (Williams et al., 2018) appear as more viable options than pure engineered

46 structures along the coast (Song et al., 2018). All the possible responses and adaptation strategies
47 should be based on updated data of the coastal state, which must be transferred to managers
48 through objective and simple indicators.

49 However, there is a lack of knowledge about the state of the beaches. Traditional techniques for
50 shoreline-change studies are photointerpretation (Pajak & Leatherman, 2002; Jones et al., 2009),
51 continuous video-monitoring (Bouvier et al., 2017; Sánchez-García et al., 2017), DGPS field
52 measurements (Pardo-Pascual et al., 2005; Psuty & Silveira, 2011; Baptista et al., 2018), LIDAR (Pye
53 & Blott, 2016) and UAV (Casella et al., 2016; Turner et al., 2016). They are limited in temporal or
54 spatial coverage, as well as being both costly and labor intensive (Do et al., 2018; Sánchez-García et
55 al., under review). Thus, the lack of continuous and up-to-date data collection systems applicable
56 homogeneously on a large scale has contributed to the lack of widespread adoption by
57 administrations.

58 In this scenario, previous works have investigated the potential of optical satellite imagery for
59 coastal surveillance. Different evolutionary studies are sustained in the identification of the
60 water/land position from free mid-resolution satellite imagery (Gens et al., 2010; Ghosh et al., 2015;
61 Luijendijk et al., 2018), mainly Landsat series (Almonacid-Caballer, 2015; Do et al., 2018). Since 2017,
62 Sentinel-2 mission offers improvements in both resolution and revisit frequency. With the
63 combination of the Sentinel-2A and 2B satellites, ESA has been providing worldwide coverage of
64 free images with a 5-day revisit. Given the large planetary coverage and high revisiting frequency of
65 the satellites, they appear as an extremely interesting source of information for studying changes in
66 coastal morphology (Castelle et al., 2015; Pardo-Pascual et al., 2014; Vandebroek et al., 2017), more
67 versatile, cheaper and simpler than videomonitoring systems. However, in order to detect relatively
68 small changes, it is necessary to overcome the coarse pixel size of the Landsat and Sentinel-2

satellites. By the moment, only a few authors have achieved the definition of the shoreline position at sub-pixel level (Foody et al., 2005; Pardo-Pascual et al., 2012; Almonacid-Caballer, 2014; Li & Gong, 2016; Liu et al., 2017; Pardo-Pascual et al., 2018). A proper definition of the Satellite-Derived Shorelines (SDS) requires to adapt the subpixel extraction algorithm to the images of the different satellites, as well as to follow an efficient workflow capable of dealing with a large volume of images. With that in mind, SHOREX system has been developed for the shoreline extraction (Palomar-Vázquez et al., 2018 a, b; Sánchez-García et al., under review). As its core, it takes the algorithmic solution for the sub-pixel extraction originally described in Pardo-Pascual et al. (2012) and Almonacid-Caballer (2014). The algorithm has been surrounded by the necessary tools for an efficient management of large volumes of mid-resolution satellite images, creating a system for automatically defining the SDS. Sánchez-García et al. (under review) assessed the accuracy of SDS on the Mediterranean beach of Cala Millor (Balearic Islands) by comparing their positions with shorelines derived from simultaneous video-monitoring. After testing the combination of different extraction parameters, the highest accuracy for Sentinel-2 imagery was defined as 3.01 m RMSE. This way, SHOREX system follows a complete and efficient workflow ranging from the acquisition of images to the definition of SDS with high accuracy. It can offer big packages of shorelines (tens per year) along large coastal areas and at the same pace in which satellite images are acquired. This poses the challenge of how to exploit the high potential of the SDS for deriving descriptors of the beach morphology. Only this way will SDS constitute an effective source of information for monitoring and understanding the coastal dynamism and thus helpful for the management of coastal areas.

The main objective of this work is to propose a methodology capable of taking advantage of high-frequency SDS data to quantify and characterize the dynamism of beaches by means of a spatiotemporal model of their widths. This approach is applied over two and a half years to 50 km

of microtidal coastline in the south of the Gulf of Valencia, evaluating the utility of the model for (1) characterizing the state of the beaches, (2) studying the impacts caused by specific events, both natural as storms and artificial as sand nourishments, and (3) locating and mapping of problematic segments.

2. METHODOLOGY

2.1. SDS and beach width definition

For this work, the data source was the freely available mid-resolution images of the satellite Sentinel-2 (S2). The analysis employed the SWIR 1 band (1565 - 1655 nm, band 11) with 20 m of spatial resolution. The images were captured in 60 different dates between 06/07/2015 and 18/01/2018, covering 925 days (Fig. 1). These are all the available images from the launch of the first of the two S2 satellites (23/06/15 and 7/03/17 respectively) until the beginning of 2018.

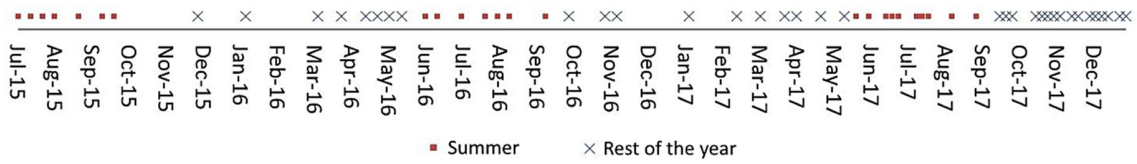

Fig. 1. Imagery employed in the analysis differentiated between summer dates (June – September) and the rest of the year (October- May).

Throughout the study period, there were small gaps caused by the existence of cloudiness. When the clouds did only affect one part of the coastal area, it was possible to take profit of the rest of the image. Nevertheless, an irregular distribution of the images appears along the year, with more available images during summer months. Therefore, the scarcity of images is remarkable along certain periods (24/09/2015 - 3/12/2015, and 17/11/2016 – 25/02/2017).

For each image (and date), Satellite-Derived Shoreline (SDS) and beach width (BW) were defined along the coast. SDS was defined as the intersection between water and land at the instant in which each image was acquired. The shoreline extraction followed the methodology described by Sánchez-García et al. (under review) and Palomar-Vázquez et al. (2018 a, b). The SHOREX system was used with a SWIR1 band, fitting a third-degree polynomial in order to detect on a 5x5 kernel the shoreline position with an accuracy of 3.01 m RMSE. The process started from an approximate line photo-interpreted from a 2015 aerial orthophotography with 25 cm resolution (PNOA, www.pnoa.ign.es). As the protocol is fully automatic the extraction efficiency increases - 8 hours of calculation time for the entire extraction workflow- while the subjectivity and bias associated with human intervention disappear. After discarding sections of shore without interest for this study (rigid structures, mouths of rivers, streams, irrigation canals, and intercalated small spaces) 41.5 km of shoreline were defined.

For defining the BW, the inner edge of the beach was defined from the same aerial orthophotography. Constituted by elements both natural (dunes and cliffs) and artificial (promenades, buildings, and roads), this inner limit is considered stable at the time scale of this work. In order to facilitate the management, the inner line of the beach was segmented into 519 segments of 80 m length. They constitute the basic spatial units on which the study has been carried out. For each segment, the shortest distance between the inner limit and the SDS was defined as the instantaneous width of the beach. Throughout the study period, 591,441 widths measurements were registered, and the average width was calculated on each date for each segment.

2.2. Spatiotemporal model of beach widths

Beach width measurements were organized and led to a continuous spatiotemporal model (Fig. 2). In order to overcome the unequal distribution of records and to have continuous records throughout space and time, BW was deduced in instants and locations without real measurements.

For this purpose, from the average width values (about 55 per segment) a TIN interpolation was carried out following the Delaunay triangulation (Tsai, 1993). Coastal segments with no width values or without morphodynamic connection were not considered for the interpolation. For a more efficient analysis, the TIN was rasterized generating the spatiotemporal model.

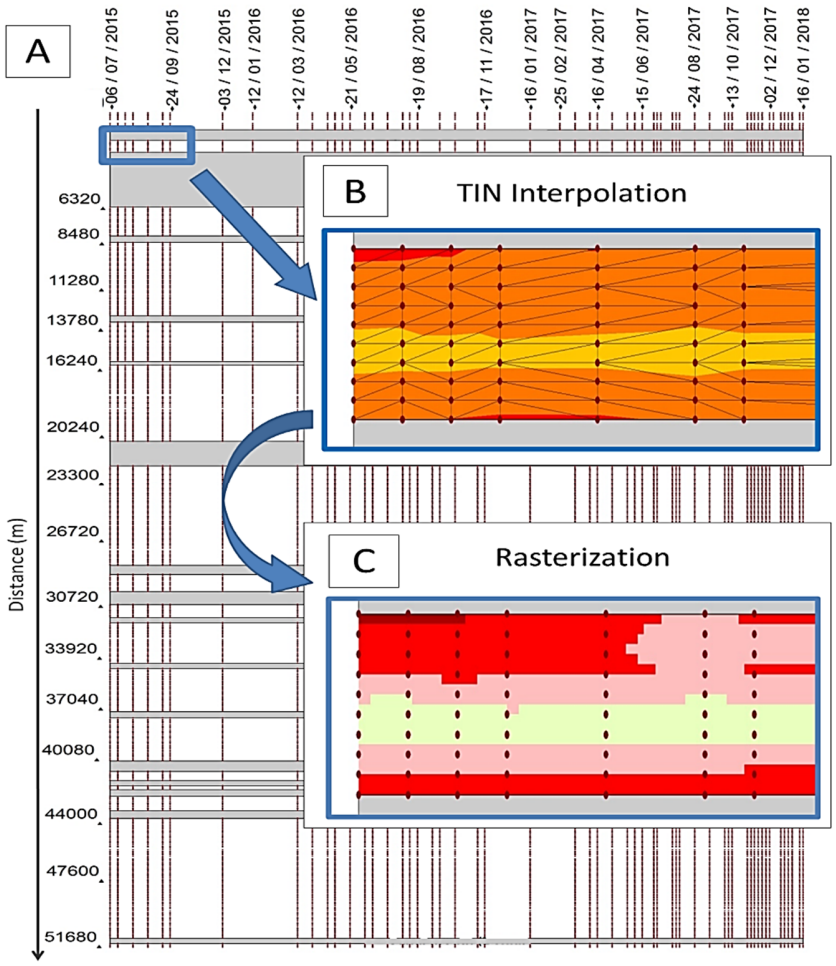

Fig. 2. Creation of the spatiotemporal model: (A) Width measurements along space (Y-axis, distance from the North) and time (X-axis, date). (B) Interpolation. (C) Rasterization leads to the spatiotemporal model: a Hovmöller diagram with 80 m and 1.2 days cells and colors representing width values. It allows identifying changes in beach morphology.

2.3. Characterization of beach state and changes

GIS analysis operations were carried out for characterizing beach state and changes in the morphology. The union of the width values of the same segment allowed defining the changes over time (925 days) in the same geographical position. On the contrary, values defined on the same date also allowed defining the width state along the whole coast.

The state of the beaches was characterized through their current width values, as well as their distribution and frequency in which they appear. The dynamism of the coastal area was analyzed through the short-term width changes that were defined by comparing an instant width with the value at the beginning of the monitored period. This way, episodes of change were detected, quantified and analyzed, trying to identify different typologies according to their magnitude and area of affection (local or large sectors). The relation between width changes and impact events as storms and artificial sediment movements was analyzed. For this purpose, the data about dumping and removal actions were integrated into a GIS in order to locate them temporally and spatially. The actions of greatest magnitude were selected and their effect was studied, as they potentially have the biggest capacity to affect the morphology of the coast and the shoreline position.

In order to identify coastal segments susceptible to experience problems in maintaining their beach functions, a minimum width threshold was defined. According to some studies on Mediterranean beaches, widths below 30-35 m may be detrimental to the development of recreational beach functions (Alemany, 1984; Yepes, 2002; Sardá et al., 2009; Jiménez et al., 2011). Therefore, the problematic segments were defined as those with a width below 30 m at least once throughout the study period. They were classified according to the number of days experiencing widths below the threshold. Furthermore, based on their locations they were grouped in different sections and sectors. According to their characteristics, the most problematic segments were identified. At the

same time, their geographical distribution was analyzed together with the coastal morphology in the surroundings, trying to get a better understanding of the cause of their problems.

3. A CASE OF STUDY FROM THE VALENCIAN COAST

3.1. Study area

The study area comprises the southern half of the Gulf of Valencia (Eastern Spain), in the western Mediterranean, the coastal segment between the Cape of Cullera and the port of Dénia (Fig. 3). Given the high anthropic and recreational pressure coupled with recent erosion problems, this sandy coast is a perfect example to apply this methodology to provide data potentially useful for coastal management.

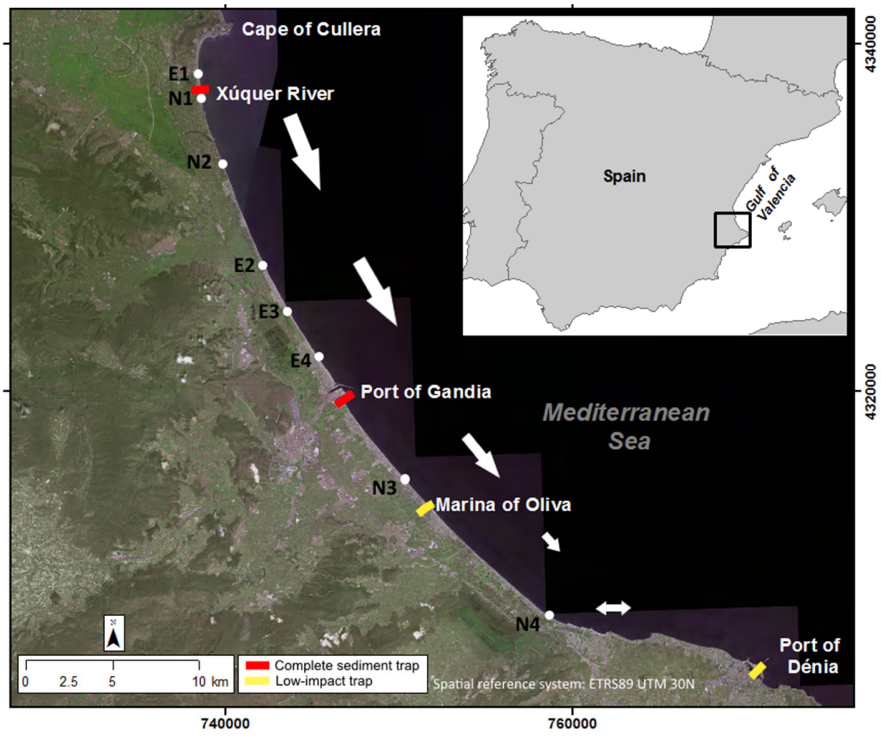

Fig. 3Littoral drift (arrows), sediment traps (squares) and artificial sand movements (points) along the study area. Extractions: E1) Sant Antoni beach, E2) Séquia la Ratlla canal mouth, E3) Vaca river

mouth, E4) Gandia beach. Nourishments: N1) South of Xúquer river mouth, N2) El Brosquil and la Goleta beaches, N3) Piles beach, N4) El Molinell beach.

It is a microtidal coast (average range of 0.3 m and maximum of 0.7 m), with significant wave height (Hs) of 0.7 m and peak period (Tp) of 4.2 s on average (Pardo-Pascual et al., 2018). During storm events waves sometimes reach 5 m (Pardo-Pascual et al., 2014) as it happens during the study period (Fig. 4), with seasonal variations showing a magnitude clearly lower than the specific episodes of high waves (always considering the microtidal Mediterranean environment). These peaks appeared mainly between autumn and the end of winter.

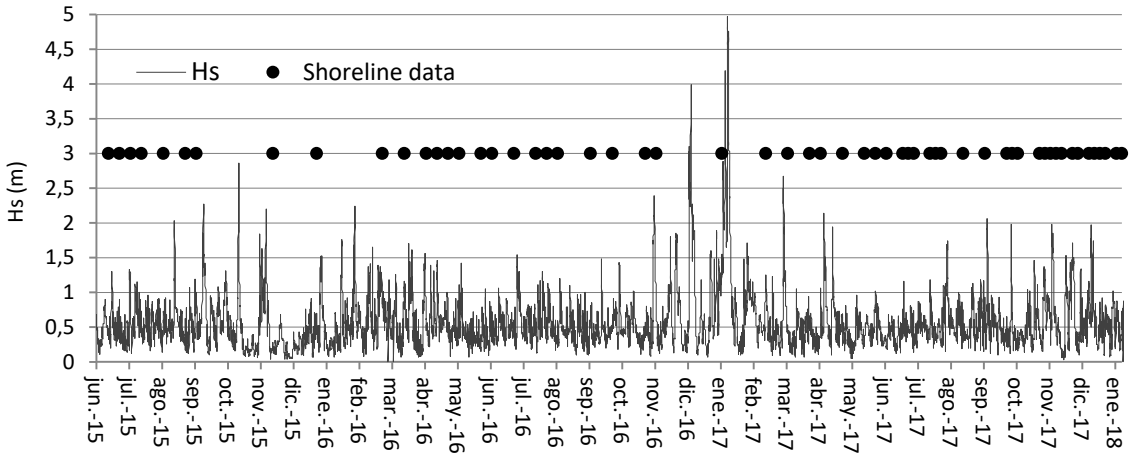

Fig. 4. Significant wave height (June 2015-January 2018) in the SIMAR point 2083108, derived from numerical modeling for deep waters by the Spanish Port Authorities (www.puertos.es). Dates with available shoreline data highlighted.

The morphology evidences a historical accumulation of sediment that allowed the development of double beach barrier and wide dune ridges (Sanjaume & Pardo-Pascual, 2003; Sanjaume et al., 2019). The region presents southerly transport caused by its orientation in combination with the direction of the waves during storms. The study area belonged to the Gulf of Valencia coastal cell

196 (between Ebro Delta and Cape of Sant Antoni, about 400 km). However, the construction of port
197 jetties has caused its subdivision in smaller coastal cells (Pardo-Pascual, 1991; Sanjaume & Pardo-
198 Pascual, 2005) as these infrastructures constitute artificial barriers for the sediment transport along
199 the coast. The most important obstacles are the jetties that protect the mouth of the Xúquer river
200 (the northern one reaches 7 m depth) and the dikes of the port of Gandia (11 m depth). In both
201 cases, they usually act as complete sediment traps, although the jetties in the Xúquer can allow a
202 by-pass during big storms. The marina of Oliva and the port of Dénia also present jetties, but they
203 are located in coastal segments with different orientations, smaller sediment transport and,
204 therefore, lower impact on the surrounding beaches. The magnitude of the longshore transport
205 varies geographically a lot: it is greater in the northern part and it decreases substantially to the
206 south, especially after the port of Gandia, and it ends south of the marina of Oliva. Finally, the
207 southernmost section does not present a clear transport direction (Pardo-Pascual & Sanjaume,
208 2019).

209 In the Valencian coast, 26% of the beaches suffer erosive processes (European Comission, 2009). In
210 the study area erosion has become a problematic issue during the last decades (Cabezas-Rabadán
211 et al., 2018; Pardo-Pascual & Sanjaume, 2019). The situation is especially remarkable because those
212 beaches constitute the basic resource for sun and beach tourism (Obiol-Menero, 2003; Cabezas-
213 Rabadán et al., 2019). Due to their recreational function, they constitute an essential source of
214 economic benefits for the Valencian region, where the tourism industry contributes with more than
215 14 % of the gross domestic product (Rico-Amorós et al., 2009).

216 As a response to coastal erosion, sand nourishment has been the defensive action most widely used
217 in recent decades (Obiol-Menero, 2003). The artificial extraction and dumping actions carried out
218 by the Administration were identified along the vast majority of the study area (Tab. 1, Fig. 3). Most

of the interventions were sand movements from sediment-surplus beaches to segments experiencing erosive problems. Between 2015 and January 2018, 191,297 m^3 of sand were extracted and 217,002 m^3 were poured. Two areas recorded the largest artificial sand movements: 72% of the sand was extracted from Sant Antoni de Cullera beach and 64% was dumped in El Brosquil and La Goleta beaches.

Table 1. Artificial sediment movements on beaches in the province of Valencia (Source: Directorate General of Sustainability of the Coast and of the Sea). Data of the southernmost 15 km of the study area (Alicante province) were not available.

Location	Municipality	Volume (m^3)	Action	Start	Finish
Sant Antoni beach	Cullera	137,489	Extraction	June-15	June-18
Séquia la Ratlla canal mouth	Tavernes/Xeraco	21,796	Extraction	March-15	May-18
Vaca river mouth	Xeraco/Gandia	8,944	Extraction	May-18	June-18
Gandia beach	Gandia	23,068	Extraction	November-17	June-18
South of Xúquer river mouth	Cullera	63,561	Nourishment	April-15	June-18
El Brosquil and la Goleta beaches	Cullera/Tavernes	138,099	Nourishment	December-15	June-18
Piles beach	Piles	14,822	Nourishment	November-15	November-17
El Molinell beach	Dénia	520	Nourishment	October-15	November-15

3.2. Results

3.2.1. Beach widths

Figure 5 shows a spatiotemporal model of the BW over the whole study area and the period analyzed, useful for understanding the beach state. All the narrow coastal segments (below 30 m) appear in reddish colors differentiated according to their magnitude. Blue and purple indicate, on the other hand, very wide segments (over 60 m and up to 159 m). Green tones represent widths between 30 and 60 m.

Wide beach segments appear located updrift of artificial obstacles to coastal transport. Their cumulative effect is associated with the progressive width increase when approaching the infrastructure as it can be seen between Séquia de la Ratlla canal and the port of Gandia, and northern of the jetties protecting the mouth of the Xúquer river. Narrow beach segments (below 30 m, red colors) appear only partially related to the interruption of longitudinal transport. In fact, a clear relationship with a sedimentary trap only appears south of the Xúquer jetties, between Brosquil breakwaters and la Goleta canal. The port of Gandia, with a strong cumulative effect on its north, clearly does not show the opposite effect on its south. Although the beach segments are quite narrow there, most of them are usually between 30 and 50 m wide. Segments narrower than 30 m have a specific but well-defined character. Fig. 6 shows the width of the beach on a given day throughout the whole study area, and narrow widths can clearly be appreciated (close to 20 m) in Bellreguard (km 25) and Piles (km 28). The 12 km in the southern end present a continuous contrast of very wide and extremely narrow beach segments (below 10 m both in km 43 and km 50).

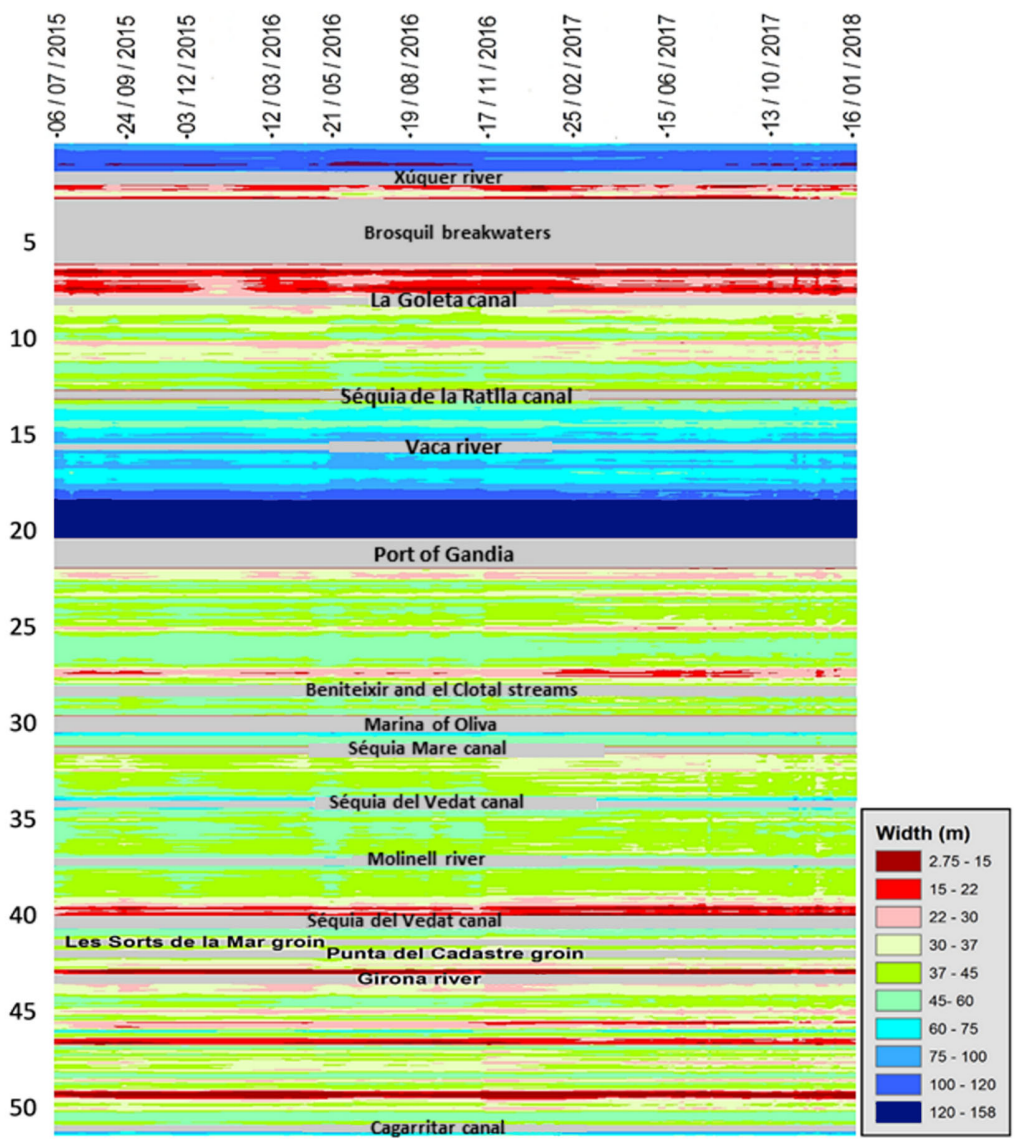

247

248 *Fig. 5. Spatiotemporal model of beach widths. Y-axis represents the location (distance from North,*

249 *in km), and X-axis the time. Cells have 80 m and 1.2 days. BW magnitude appears in different*

250 *colors. Segments not considered appear in grey.*

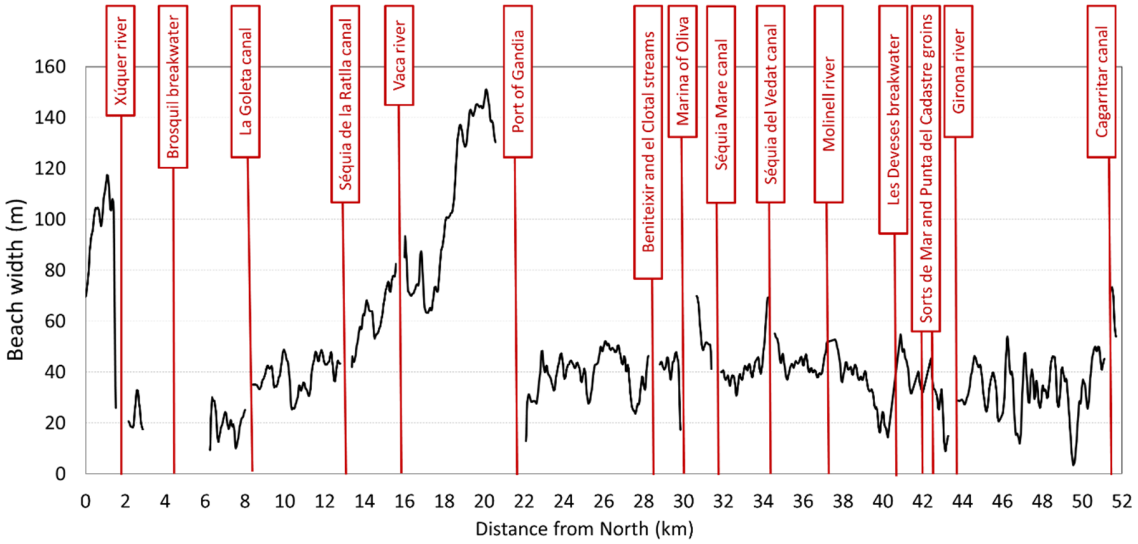

Fig. 6. Beach width along the study area on 17/11/16. Infrastructures, rivers, and canals highlighted.

Figure 7 shows a strong asymmetry in the BW distribution. Although the widths range between 3 m and 159 m, only 11.45% of the beach segments are wider than 80 m. More than a half (55.5%) have between 30 and 50 m. The percentage below 30 m reaches 15.9%, while 2.1% are critical below 15 meters. Nevertheless, these data hide the variation along time: when considering the summer dates of the different years important variations appear in the percentage of beach segments narrower than 30 m meters (14.76 %, 14.34 % and 17.62 % for 2015, 2016 and 2017 summers respectively).

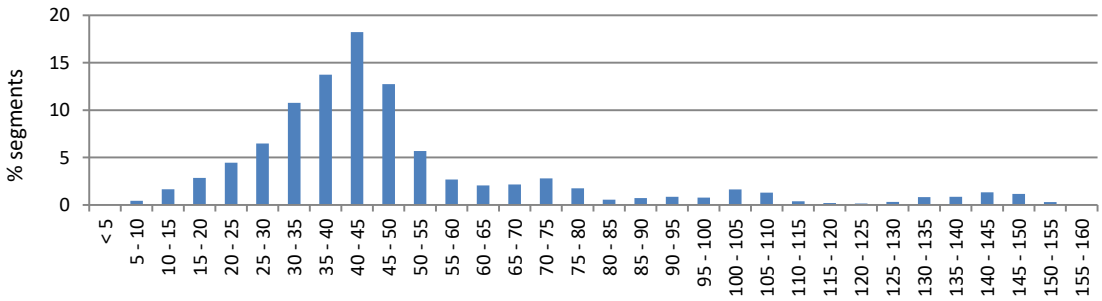

Fig. 7. Histogram of widths registered in the different segments of analysis.

3.2.2. Beach changes

Short-term beach changes were characterized along the study period by comparing the instantaneous width of each segment against the width on the first date analyzed. Fig. 8 shows a spatiotemporal model that simultaneously represents all the changes. There was a predominance of width loss processes (yellow to red). The average change for the whole study area is -3.4 m, with the first three quartiles registering negative values. Fig. 9 shows a distribution of the types of changes that resembles a normal curve but with a clear negative bias. Changes between -3 and -4 m are the most abundant (13%).

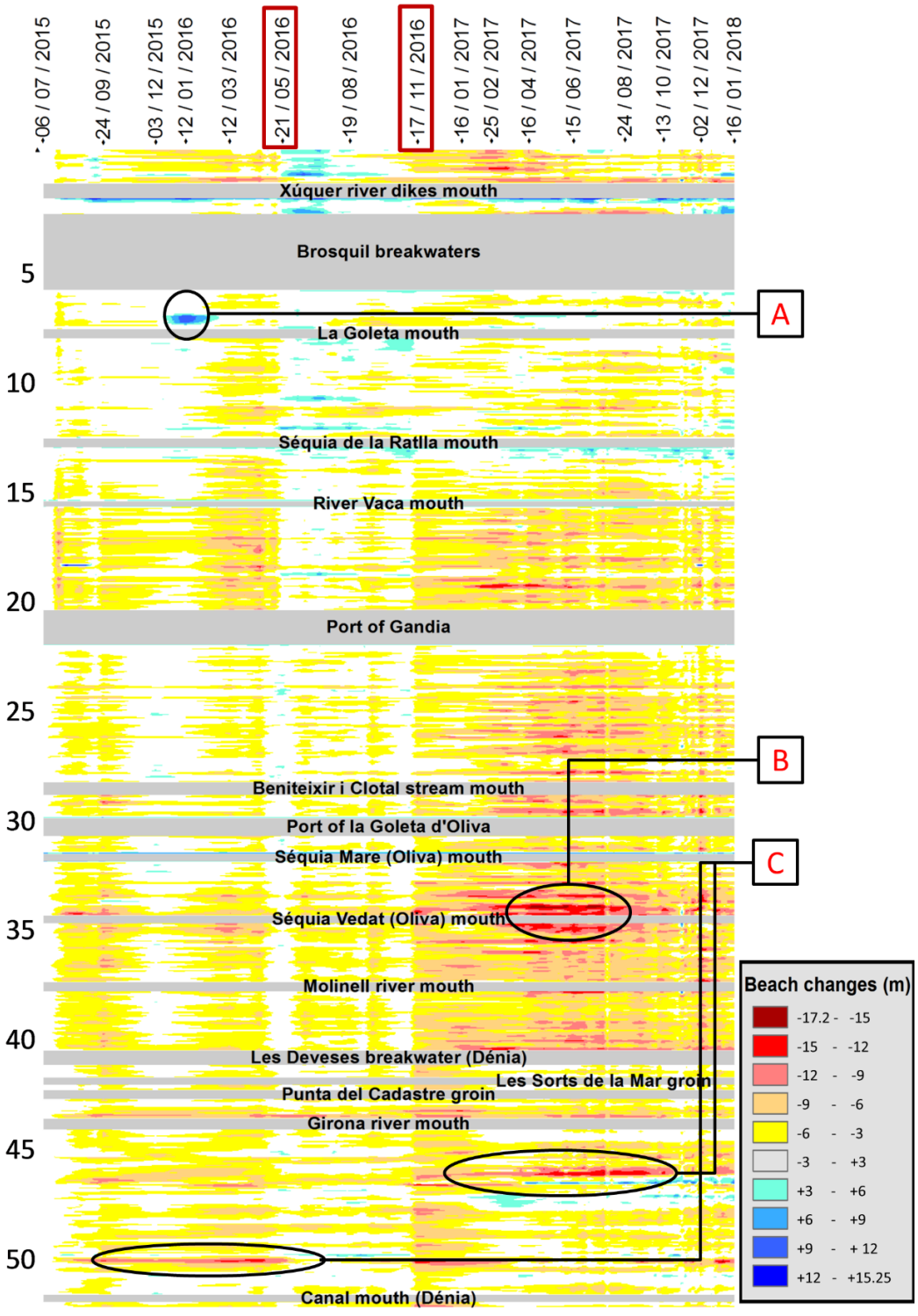
-06 / 07 / 2015
-24 / 09 / 2015
-03 / 12 / 2015
-12 / 01 / 2016
-12 / 03 / 2016
-21 / 05 / 2016
-19 / 08 / 2016
-17 / 11 / 2016
-16 / 01 / 2017
-25 / 02 / 2017
-16 / 04 / 2017
-15 / 06 / 2017
-24 / 08 / 2017
-13 / 10 / 2017
-02 / 12 / 2017
-16 / 01 / 2018
Xúquer river dikes mouth
Brosquil breakwaters
La Goleta mouth
Séquia de la Ratlla mouth
River Vaca mouth
Port of Gandia
Beniteixir i Clotal stream mouth
Port of la Goleta d'Oliva
Séquia Mare (Oliva) mouth
Séquia Vedat (Oliva) mouth
Molinell river mouth
Les Deveses breakwater (Dénia)
Les Sorts de la Mar groin
Punta del Cadastre groin
Girona river mouth
Canal mouth (Dénia)
5
10
15
20
25
30
35
40
45
50
A
B
C
Beach changes (m)
-17.2 - -15
-15 - -12
-12 - -9
-9 - -6
-6 - -3
-3 - +3
+3 - +6
+6 - +9
+9 - + 12
+12 - +15.25

271

Fig. 8. Changes along the study area (distance from North, in km). Width on 6/07/2015 as a reference. Three episodes of local change (A, B, C) and general changes in 21/05/2016 and 17/11/2016 are highlighted.

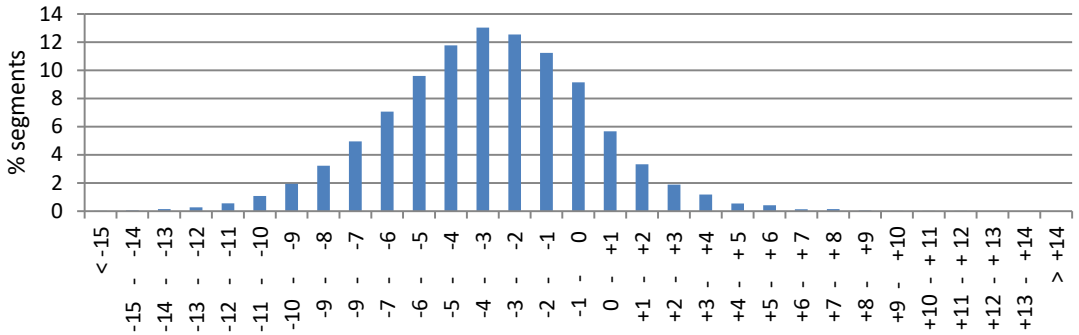

Fig. 9. Beach changes and their direction

Width changes showed different magnitudes and directions in space and time (Fig. 8). At least two particular episodes caused short-term changes that affected large portions of the study area, although with different magnitudes. Figure 10 shows in detail the magnitude and direction of the width changes associated with these two episodes. For each one, the width was compared between two dates, associated with the start and end of the episode respectively.

The first episode took place approximately on 21/05/2016 and had positive values, with beaches generally widening. The changes did not affect the whole study area but were reflected in the 20 km further north of the study area and in the last 4 km to the south (Fig 8, 10). It took place at the end of a calm period (Hs was below 1 m for approximately 20 days, Fig. 4).

The second episode occurred around 17/11/2016 and it was even more evident because it affected the entire study area (Fig 8, 10). On the contrary, it clearly presented negative values, and the majority of the segments registered erosion. The changes were negative for the whole area (mean regression of -3.5 ± 1.8 m), which suggests a general cause affecting the whole coast. This episode

occurred associated with a storm (Hs reached 2.32 m on 15/11/2016, Fig. 4) that could be considered the first important one of that autumn. Similarly, other episodes seem to show a general response to the changing oceanographic conditions. This is the case of a recovery process along December of 2015, a long period without high waves.

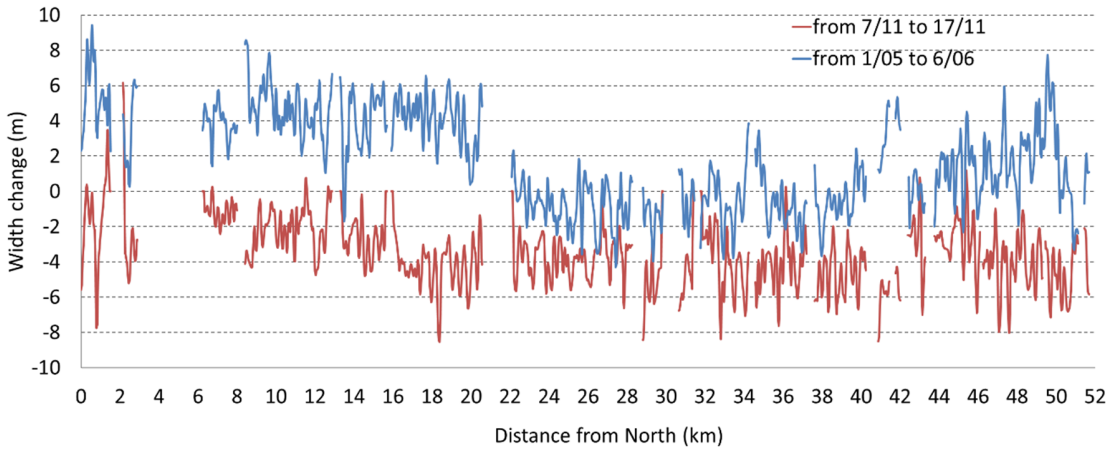

Fig. 10. Short-term width changes associated with two specific episodes: 21/05/2016 and 17/11/2016. The changes were quantified between 1st of May and 6th June (blue) and between 7th and 17th of November (red).

The detailed analysis of the change model (Fig. 8) also made it possible to recognize changes on a local scale, with a much smaller spatial dimension. Three types of local change episodes have been differentiated:

(A) Those with an inverse tendency to the one observed in close areas and even in the same spot at another time. The clearest example is the one observed in position A (focused on km 8) associated with a strong widening of the beach (up to 10 m) around on 12/01/2016.

(B) Those affecting an entire sector, and although obvious, they are not excessively punctual either in space or time. Thus, it is possible to recognize the places and moments in which the changes were of greater magnitude. As an example, North and South of Séquia del Vedat

canal between 18/03/17 and 13/10/2017, we can see setbacks of about -15 m with respect to the initial situation and this substantial alteration was maintained for months.

(C) Those in which it is possible to simultaneously identify completely opposite dynamics in very near locations. The example is paradigmatic since, on the same beach, a 13 m recession took place while, at a distance of only 400 m, an advance of 10 m was registered.

Short-term changes linked to artificial sediment mobilization were also analyzed. The analysis was focused on the two beaches that registered the major actions of sand removal and dumping (Fig. 11, 12). On Sant Antoni beach (Cullera) 137,489 m^3 of sand were dredged between June 2015 and June 2018. On the contrary, 138,099 m^3 were used for the nourishment El Brosquil and la Goleta beaches, in which actions started in December 2015 and were repeated in the next winters.

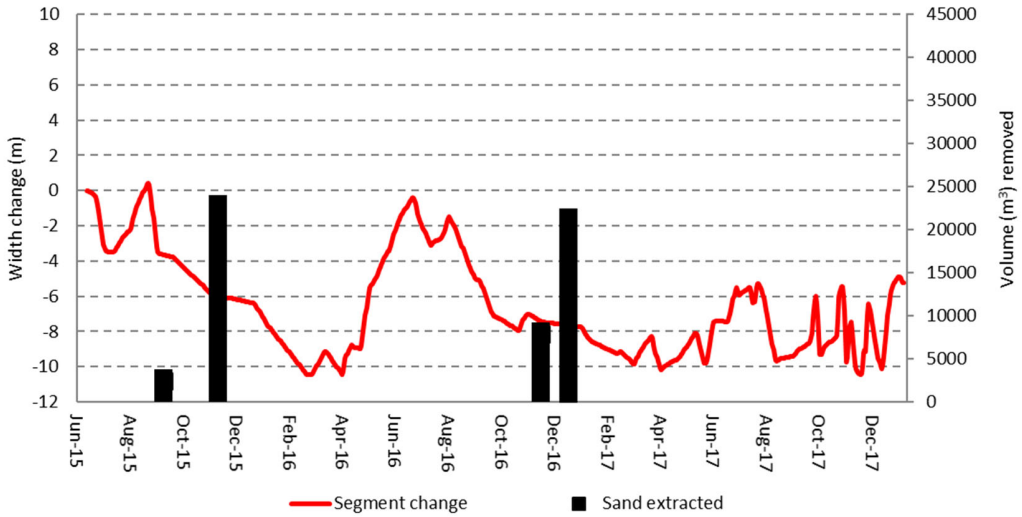

Fig. 11. Sand extractions in Sant Antoni beach (Cullera) and width change in the associated 80 m segment (red).

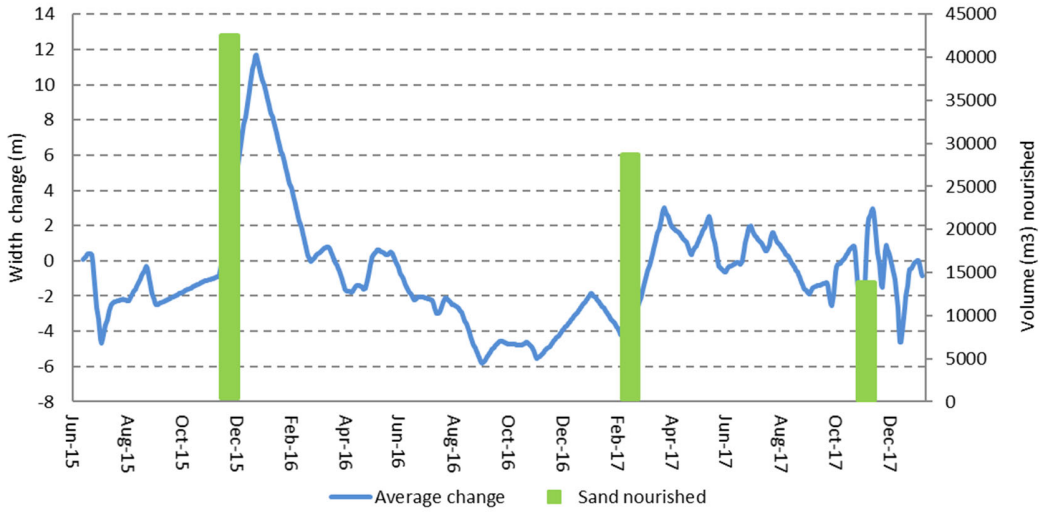

321

322 *Fig. 12. Sand nourishment (green color) in la Goleta beach (Tavernes) and the associated width*

323 *change of the beach (blue).*

324 The effects on the width were clear in both cases. On the one hand, regression episodes were
325 registered coincident in time with the sand removal activities. Width loss took place on the whole
326 beach, especially remarkable in one of its segments. On the other hand, la Goleta showed accretion
327 episodes coincident with three different sand nourishments. The first one, the most remarkable
328 (41,600 m^3 about 15 December 2015), was associated with a positive mean change of the shoreline
329 of around 12 m. It can be clearly seen in the spatiotemporal model as a local change episode (Fig. 8,
330 A). A second action (27,800 m^3 at beginning of March 2017) was followed by a positive mean change
331 of more than 6 m. Finally, a smaller nourishment (12,830 m^3 about 15 November 2017) seemed to
332 be associated with a positive change close to 4 m.

333 ### 3.2.3. Problematic narrow segments

334 Beach segments with insufficient width and therefore likely to cause conflict with beach functions
335 were identified. At least once along the study period, 15.2% of the analyzed segments registered a
336 width below 30 m, while 1.5% showed a critical situation below 15 m.

337 The amount of time experiencing a problematic narrow situation varied a lot between segments
338 (Tab. 2), and it was used to classify them. Along the study area, a width below the 30 m threshold
339 was registered continuously along 3.84 km, while it was maintained more than 75% of the time
340 along 2.16 km.

341 *Table 2. Classification of beach segments with problematic width according to the proportion of*
342 *measurements lower than 30 m throughout the study period.*

Percentage of days	Code	Length (m)
1%-25%	5	3840
25%-50%	4	1440
50%-75%	3	640
75%-99%	2	2160
100%	1	3840

343 Problematic segments appeared grouped in three large coastal sectors with different orientation
344 and characteristics (Fig. 13). The first one, Sector 1, appeared southern of the Xúquer river along 9.7
345 km, with an orientation NNW-SSE. Sector 2 appeared along 11.5 km and with NW-SE orientation
346 between the port of Gandia and the beaches south of the marina of Oliva. Sector 3 appeared at the
347 southern end of the study area, along 10.5 km of Dénia coast, oriented W-E (100º). At the same
348 time, inside these three large sectors, several problematic segments (with width records below 30
349 m) appear arranged continuously (or almost) along the coast. When grouping these segments it is
350 possible to identify 19 sections with problematic situations that cover up to 13.36 km (although few
351 segments were not identified as problematic).

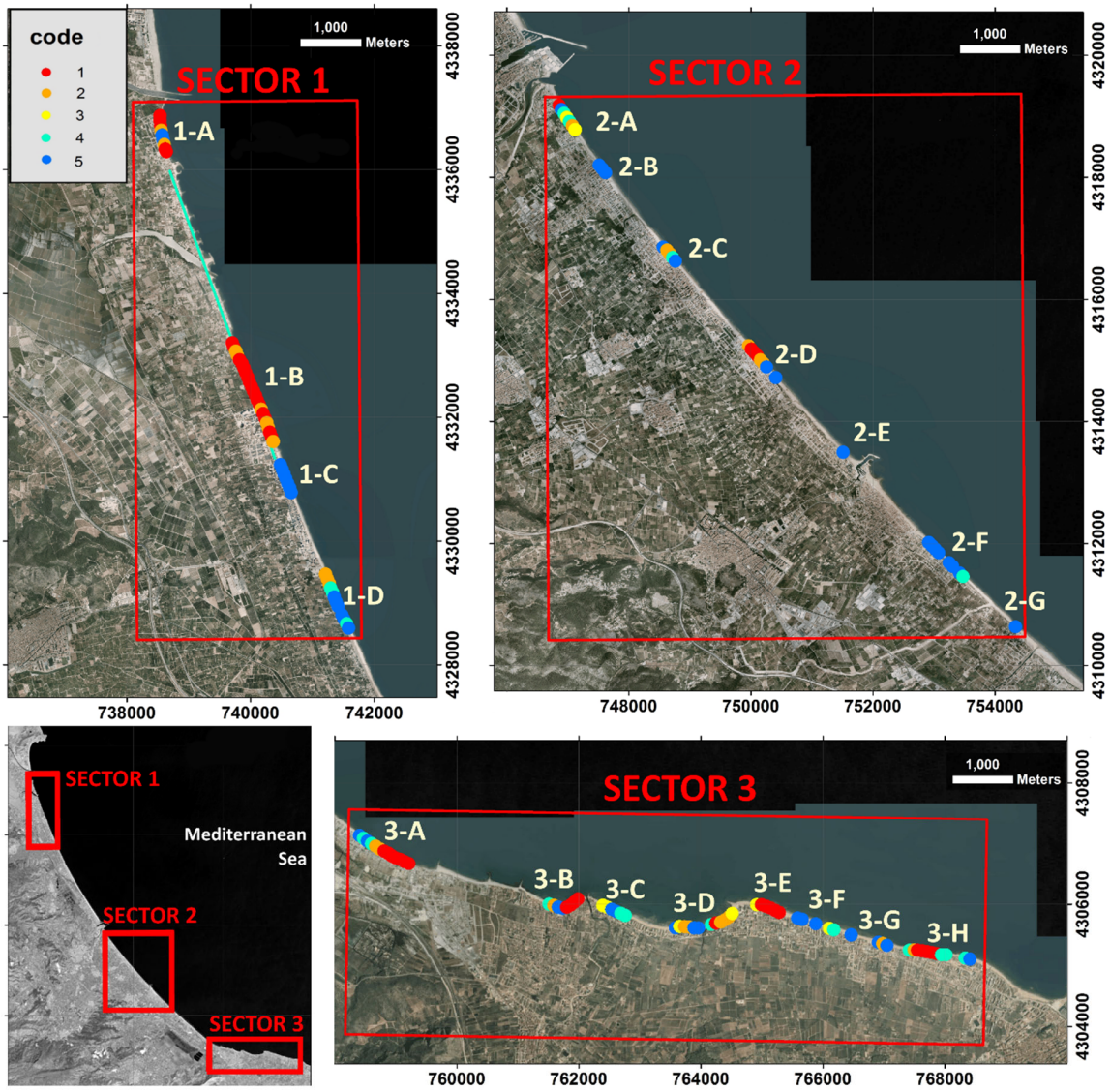

352

353 *Fig. 13. Geographical distribution of the problematic segments classified according to the*

354 *percentage of days registering BW below 30 m. They appear grouped in three large sectors. A line*

355 *in cyan shows a long rigid segment not included in the analysis. More detailed information is*

356 *included as supplementary data.*

357 Sections 1-A, 1-B, 3-A, 3-B, 3-E and 3-H present average widths below 30 m over the entire period.

358 Among them, as particularly problematic appear the section 1B (Brosquil and la Goleta beaches)

359 with the narrowest average width (21.5 m) along 1.8 km, and 3-H with the narrowest segment (6.6
360 m).

361 Sector 1 (9.7 km) is located south of the Xúquer river dikes and includes four sections covering 4.16
362 km of beach with an average width of 26 m. Sections 1-A and 1-B are the narrowest ones and,
363 between them, there is a coastal stretch with artificial structures (seawall, breakwaters and small
364 groins) that aim to stop the erosion. Section 1-B (Brosquil and La Goleta beaches), located downdrift
365 of the artificially protected area, is the longest of all the areas studied (1.84 km) and the one with
366 the smallest average width (21.5 m). Section 1-C shows substantially greater widths (33.4 m on
367 average), and it is separated from 1-B by a small structure protecting the mouth of an old inlet that
368 connects with the wetland.

369 Sector 2 (11.7 km) includes seven sections with extremely variable dimensions. In general, the
370 segments are wider (32.9 m average) than in the other sectors and there is a smaller proportion of
371 problematic segments. In fact, only 22.4% of the segments in this sector have at some point widths
372 below the 30 m threshold. Problematic sections show three different typologies in relation to the
373 presence of obstacles and rigid structures. (i) Sections located downdrift of an obstacle. That is the
374 case of section 2-A (0.5 km length) south of the port of Gandia with an average width of 30.6 m. (ii)
375 Sections linked to artificial rigid structures too close to the shoreline spatially constraining the beach.
376 That happens with sections 2-B (0.18 km length) in Daimús beach, 2-C (0.37 km) in Bellreguard beach
377 and more remarkably in 2-D (0.7 km) in Piles beach (26.8 m average). (iii) Sections not associated
378 with obstacles or structures as 2-E, 2-F, and 2-G. Section 2-F, the largest one, extends 0.85 km with
379 an average width is 35.4 m but at various times has recorded widths less than 30 m. It should be
380 noted that its inner edge is largely constituted by dunes.

Sector 3 (6.16 km) has an average width of 28.78 m, 8 problem sections. Although the sector presents great heterogeneity of typologies, 47.7% of the segments at some point have presented less than 30 m. The segments with the greatest problems have been analyzed in depth (Fig. 14). In several cases they show a punctual sedimentary deficit linked to artificial or natural barriers to the littoral drift, as it happens in 3-A, B, C and D. In section 3-A, the width increases from the jetty progressively towards the west. Sections 3-B and 3-C show very narrow beach segments at the fan-delta of the Girona river, which widen to the east and west. Section 3-D shows a beach supported by the Punta dels Molins breakwater, which most problematic point may remain narrower or unsupplied depending on the direction of transport.

However, sections 3E and 3H show no barriers to transport, and therefore the cause of the problems does not seem clear. In the case of section 3H, given the possible relation with the artificial occupation of the active beach, an analysis from a historical perspective was carried out. For that purpose, a 1956 orthophotography was combined with recent shoreline positions and the current inland limit of the beach (Fig. 15). The analysis determines that the current inland border coincides with the one existing back in the 1950 decade when the beach was already extremely narrow.

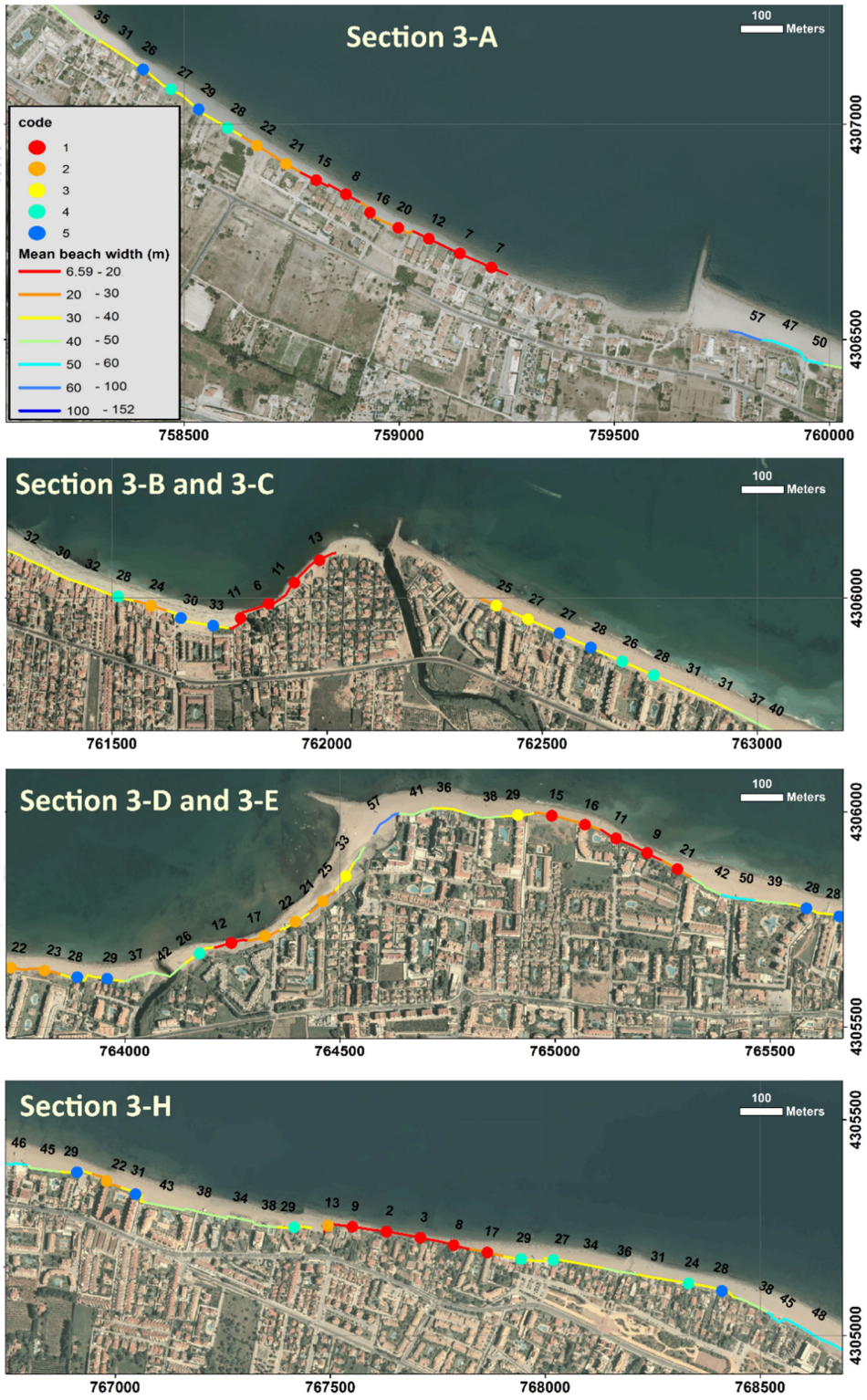

397

398 *Fig. 14. Problematic sections. Different colors represent the percentage of days with widths below*

399 *30 m and the mean beach width, and the numbers show the minimum width recorded.*

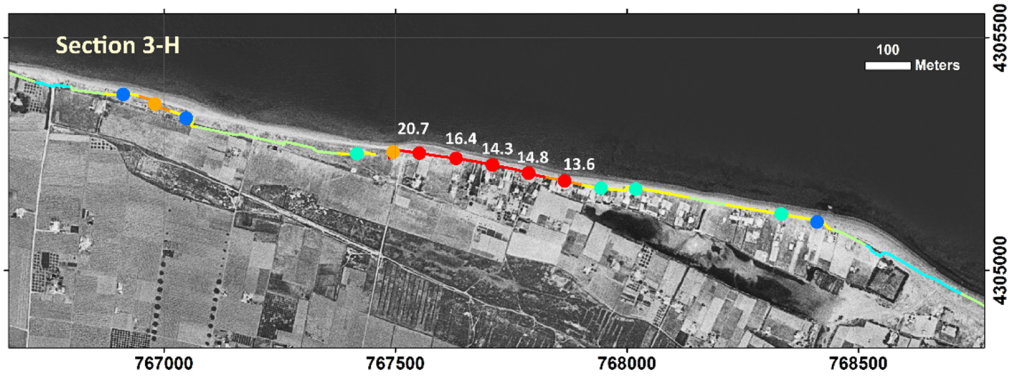

Fig. 15. Orthophotography with 0.5 m resolution created by the Valencian Cartographic Institute (ICV) from a photograph from May 1956. The inner edge of the current beach appears overlayed with the percentage of days with widths below 30 m, as well as the minimum width recorded.

4. DISCUSSION

This study shows the potential of applying a large package of Satellite-Derived Shorelines (SDS) for monitoring large coastal sectors. The extraction algorithm and the automatic protocol SHOREX developed in previous works (Pardo-Pascual et al., 2012, Almonacid-Caballer, 2014; Sánchez-García et al., under review) constitute a time-efficient solution for this purpose. It may supply up-to-date information at a regional scale at the same pace as satellite platforms acquire the images. This has made possible to monitor the shoreline position along the Valencian coast using 60 records for a period of two and a half years.

Starting from Sentinel-2 mid-resolution images, SDS are defined with great accuracy –RMSE 3.01 m. Although other data acquisition methods such as video-monitoring may obtain higher accuracies they do not possess the large spatial coverage offered by satellite imagery. From SDS, beach widths are derived as an intuitive indicator of the punctual state of the beaches on micro-tidal environments. The raster model organizes a large amount of morphological information in the spatial and temporal continuum. This model makes it possible to characterize the beach state and to identify narrow segments that may conflict with beach functions. The possibility of visualizing in

great detail the changes throughout space and time facilitates their interpretation. It allows the analysis of short-term changes and their relationship with both natural events and human actions. Thus, it is possible to identify episodes that affect large sections of the Valencian coast and to differentiate them from those local, as well as making an approach to identify their causes.

Results show a relation between major width changes and wave conditions. High-energy episodes have repercussions over large areas causing beach retreatments. On the contrary, calm periods seem to result in seaward movements of the shoreline and beach recovery. This dynamic is well known and is associated with changes in the morphology of the beach profile (Jara et al., 2015). The proposed methodology makes it possible to quantify the changes and measure the different response of each beach. In other cases, wave conditions seem to present more local impacts, to which should be added other elements such as the coastal orientation and the incident waves, the distribution of anthropogenic obstacles, as well as the accumulation of different storm episodes, that should be considered for a deeper analysis. Previous works had already shown the possibilities that SDS offer for recognizing the unequal response to storms due to the local factors that modulate those impacts (Pardo-Pascual et al., 2014; Cabezas-Rabadán et al., 2018). However, the availability of a greater number of data per year and the methodological improvements implemented in the SDS definition process (Sánchez-García et al., under review) allow a more robust and reliable definition of the coastal response.

Defining the shoreline position by satellite imagery during the maximum impact of the storm is a difficult task due to the usual cloud cover. Radar images could be an alternative, but the evaluations carried out show lower precisions (Lubczonek, 2017). Another strategy consists in modeling the behavior of the beach and foreseeing the response. This requires calibrating the model with real data about the morphological change, which can be obtained by topo-bathymetric surveys (Yates

et al., 2009) or video-monitoring (Jara et al., 2015). For these calibrating purposes, it has recently been demonstrated that SDS are equally effective than video-monitoring (Jaramillo et al., under review). Thus, SDS could potentially be used to test and adjust the models in many more areas generalizing their applicability.

The response to actions more limited in space and time as sand extractions and nourishments was studied on two beaches. Despite the absence of in situ high precision measurements, it is possible to identify changes coincident in space and time with sediment movements. It is important to remark that in both cases and unlike other previous works (Vandebroek et al., 2017; Hagenaars et al., 2018; Pardo-Pascual & Sanjaume, 2019; Cabezas-Rabadán et al., 2018) the detected changes are associated with actions of very small magnitude. Thus, in contrast with the movement of 252,000 m^3 of sediment previously detected in this same coast (Pardo-Pascual & Sanjaume, 2019), now it has been possible to detect movements even below 15,000 m^3. The results prove that this type of actions can be identified with the SDS. At the same time, it is possible to monitor the effects in the surrounding area and the durability of the action (and therefore, the investment made). It is well known that anthropogenic actions influence the state and behavior of beaches (Sanjaume & Pardo-Pascual, 2005; Pagán et al., 2016, 2017; Stronkhorst et al., 2018). In light of sea-level rise, nourishment actions appear as a common solution for the beach loss preventing shore retreat (Stive, et al, 1991). Sometimes beach retreatment events lead managers to take hasty decisions with insufficient data. Nevertheless, these actions have an important cost and environmental impact (Peterson and Bishop, 2005; Speybroeck et al., 2006) and the benefits may be of short duration (Cabezas-Rabadán et al., 2018). The real effects of these interventions are generally not monitored and well defined. It is essential to quantify their effect on space and time. This is the only way to assess the cost-benefit for society, and thus be able to support critical decision-making by managers.

SDS seem to serve this purpose and could be applied for monitoring both large-scale sectors punctual segments, allowing assessing the environmental impact of specific actions.

The spatiotemporal models allow characterizing the state of the beaches and its problematic segments with higher frequency and more rigorously than only a few specific measurements. This makes it possible to identify in advance sectors likely to conflict with beach functions. It may be used for identifying segments without a sufficient width for sustaining the recreational use of the beach, or for protection purposes at the arrival of the storm season. This is important as pre-any-crisis event management is very advantageous compared to crisis management, which entails high risk and cost (Williams et al., 2018). Following the criteria of the literature, the recreational function may be especially affected in beaches below a 30 m threshold. Taking advantage of continuous measurements, segments narrower than 30 m at least once along the study period were identified as problematic. They represent a significant percentage of the coast (15.2%), while only a small percentage show a critical condition (1.5%). This is in line with the Valencian erosive trend over the last decades (Pardo-Pascual, 1991; Sanjaume & Pardo-Pascual, 2005; European Commission, 2009). Moreover, the results have evidenced that storm events can strongly affect the available width for recreational purposes as demonstrated in 2017 summer, after the 2016-17 winter storms, when the percentage of beaches too narrow for the maintenance of this function increased 3.28 %.

The analysis of problematic segments in its geographical context makes it possible to define specific problematic typologies as well as offering hints to the causes of imbalances in sediment distribution. Firstly, there is a clear relation between widths and sedimentary traps due to the N-S transport along the larger coastal cell. Barriers to longitudinal transport cause local sediment shortages (sections 2-A, 3-A, 3-B, 3-C and 3-D, Fig.13,). In some cases, seawalls built with the aim of stopping erosive processes (sector 1) appear linked to erosive problems downdrift. These results are consistent with

488 previous studies that show that high anthropogenic pressure has degraded greatly the littoral and
489 contributed to a significant coastal regression (Yepes & Medina, 2005; Obiol-Menero & Pitarch-
490 Garrido, 2011).

491 Natural causes also bring sediment imbalances. As an example, the fan-delta created by the Girona
492 river (sections 3-B and 3-C in fig. 14) causes a punctual coastal progradation (Segura-Beltrán &
493 Pardo-Pascual, 2019) evidenced by the subsequent displacement of sediment away on both sides.
494 The mouth marks a turning point, the edge of a small sedimentary cell. The west coast of the fan
495 delta shows smaller widths as it is not being fed by longitudinal transport under practically no
496 circumstances. The waves from the west that would provide sand towards that point do not have
497 sufficient fetch as the wave height is minimal and the magnitude of the transport is practically non-
498 existent. On the contrary, although the east face also is deficient, in some cases it may receive sand
499 form eastern beaches, basically during NE storms.

500 In recent decades, the coastal urbanization process has led to the construction of artificial structures
501 too close to the shoreline (Obiol-Menero, 2003), constraining the beach and preventing its natural
502 readjustment (Fig. 13, 2-B, 2-C y 2-D). This would also be the case of section 3-H, where the
503 occupation of the waterfront several decades ago left doubts with regard to the cause of the
504 narrowing. The evolutionary analysis of the morphology of the coast shows that the inner edge of
505 the beach coincides with that of the 1950s when the beach was already extremely narrow (Fig. 15).
506 The cause of the problems in that section is therefore very probably due to the construction of
507 houses fixing the inner limit of the beach before 1956. In this case, the “problem” remains for
508 decades because in fact the beach area has been artificially occupied. Segment 3-E also presents
509 constricting urbanization, but the presence of rocky outcrops close to the shore plays an essential
510 role as natural protection for the shore: waves break at a certain distance impeding a freely

sedimentary transport and minimizing beach mobility. By this reason, the beach width remains much more stable than the segment 3-H.

Problems in segments 2-E, 2-G and especially 2-F seem not to be related with the previous causes: they suffer neither the interruption of the downdrift nor the occupation of the beach system (in fact, they present a well-developed foredune) (Fig. 13). Furthermore, during the last centuries, the sector has globally experienced a clearly cumulative trend as evidenced by a double beach barrier and archaeological remains (Pardo-Pascual & Sanjaume, 2003; Sanjaume et al., 2019). In contrast, recent changes indicate the existence of a stable or slightly recessive dynamic (Sanjaume & Pardo., 2007). This work also states that the sediment size has suffered a slight increase with respect to the mid-'80s (Sanjaume, 1985) mostly linked to an erosive trend. The existence of excessively narrow segments to the south of the marina of Oliva (2-E, 2-F, 2-G) reinforces this idea. Figure 16 shows problematic segments with retreatments over 10 m: precisely the sector with greatest losses coincides with the problematic segments in Oliva. These results suggest that the monitoring method used is sufficiently refined to detect erosive trends, even if they are still very tenuous.

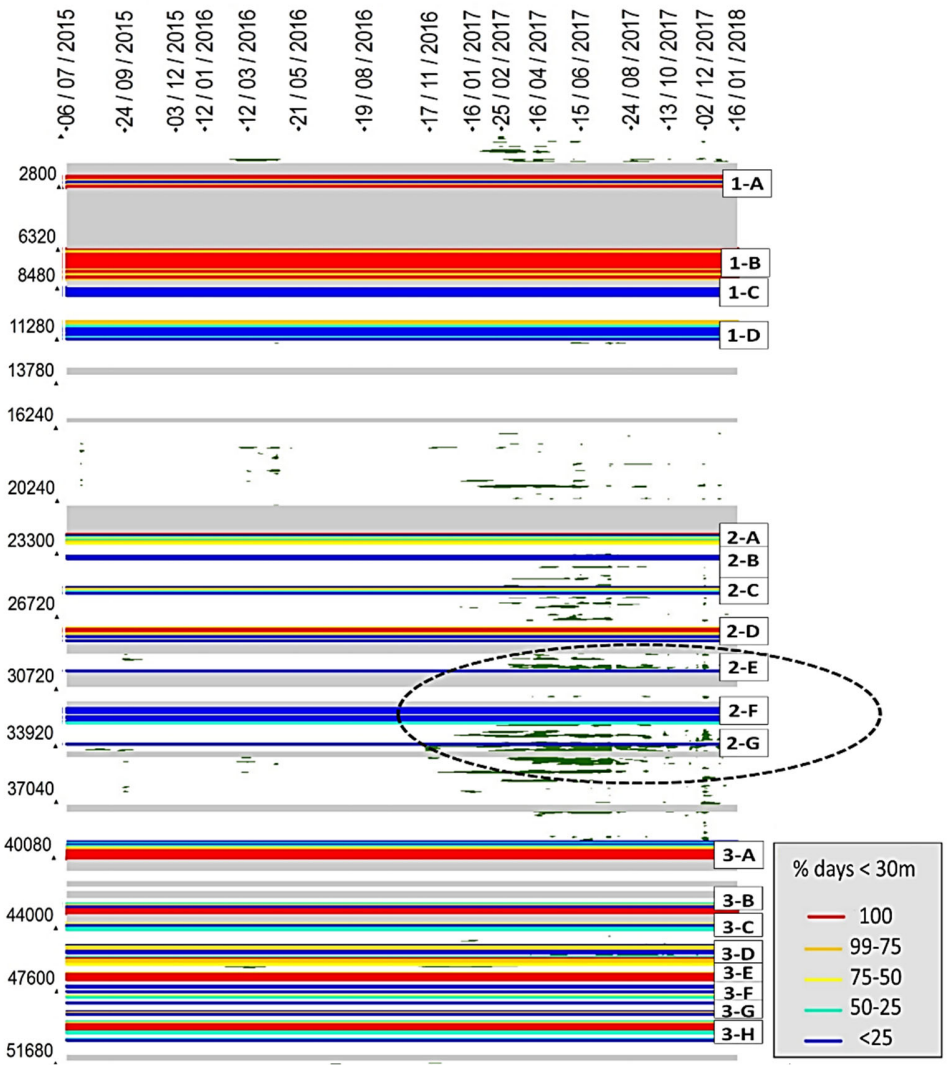

525

526 *Fig. 16. Shoreline retreatments greater than 10 m with respect to its initial position (dark green). At*
527 *the same time, % of days in which the segments are narrower than 30 m.*

528 Continuous and large-scale monitoring of the morphological changes of the coast through indicators
529 as shoreline position and beach width is fundamental for understanding coastal dynamics (Song et
530 al., 2018). It may fill the shortage and fragmentation of available long-term data (Defeo et al., 2009)
531 providing the holistic and homogeneous approach required by coastal monitoring systems,
532 facilitating the analysis of changes and the subsequent management (Cabezas-Rabadán et al., 2019).

If the erosive trend continues in the Valencian coast narrow sectors will expand affecting the beach functions. Among them, the recreational one constitutes the major concern for coastal managers (Micallef & Williams, 2002). This is especially remarkable along the area of the case study, where the management of most of the beaches is oriented for sustaining recreational activities as sun and beach tourism plays a huge role in the economy (Cabezas-Rabadán et al., 2019). In fact, the regional Administration has just started using the beach width in order to organize the beach exploitation through the Territorial Action Plan for Green Coastal Infrastructure of the Valencian region (GVA, 2018). The sea level rise is likely to put beach functions at risk, and it will further force coastal areas to take measures. Planned retreat seems to be the most viable solution, especially in regions where engineered structures can destroy the tourism-related industry (Song et al., 2018). Nevertheless, this type of measures require reliable data of the coastal state, and there is a shortage of means to obtain them, especially remarkable in developing countries (Saleem & Awange, 2019). In such cases, obtaining data from satellite imagery appears even more suitable given its cost-effective approach.

Among the limitations of this methodology, one of the severest constraints appears linked to the number of days with satellite images and, therefore, available data. At the same time, given the influence of clouds, there is an irregular distribution of images along the year, higher in the summer months. All this influences the study of the response of beaches to specific actions and episodes since in microtidal beaches the recovery can take place in a few days (Ranasinghe et al., 2012) making the changes unnoticed if it occurs in periods with no available data. However, the available Sentinel-2 (5 days of revisit time) can potentially be combined with Landsat 8 images resulting in a scenario with very low revisit intervals (average of 2.9 days combining both platforms according to Li & Roy, 2017).

About the accuracy when defining SDS, assessments with real data hardly appear in the literature (Do et al., 2018). Nevertheless, Sánchez-García et al. (under review) estimated the accuracy of this methodology from Sentinel-2 images by comparing with simultaneous in situ and independent observations on a Mediterranean microtidal beach similar to those studied in the present work. It gives credibility to the method and delimits its potential usefulness. The obtained SDS accuracy is considered more than sufficient to record the magnitudes of the changes with the necessary degree of certainty for the purposes of this paper. The water/land indicator of the shoreline position presents uncertainty associated with punctual changes generated by oceanographic variables such as waves and tides. This effect has been minimized due to the conditions of the Mediterranean coasts, as well as due to the availability of a more or less continuous series of data. Nevertheless, bearing all this in mind, and in the absence of assessments on coasts with different tidal levels, the application of the methodology in meso and macro-tidal coasts would not be immediate. Likewise, the width as beach state indicator may be meaningless on changeable environments.

5. CONCLUSIONS

The availability of SDS obtained from Sentinel-2 with high frequency and sufficient degree of precision poses the challenge of taking advantage of this new source of information to improve knowledge of the morphology and dynamics of the beaches. This work offers a methodological proposal based on the measurement of the width in short beach segments (80 m long) using the SDS and the inner limit of the beach. From these data, a spatiotemporal model of the beach widths and their changes was created for easy consultation of the coastal state and the dynamism of the microtidal beaches at different spatial and temporal scales.

The methodology has been applied along 50 km of the Valencian coast, as it constitutes a representative example of a coast highly exploited and modified by the human being, and threatened by erosive processes. Results show how the methodology is able to characterize changes

579 in the shoreline position in response to both natural events and artificial actions, either locally or in
580 large regions. It has been demonstrated that even small-magnitude sediment movements create
581 perceptible changes in beach width –only 12,830 m^3 caused 4 m width increase--, evidencing the
582 potential of SDS and other derived morphological indicators as tools for monitoring the effects of
583 anthropogenic actions. At the same time, SDS are also able to register the beach response to natural
584 events. Storm episodes exceeding certain magnitudes create general shoreline retreatments, with
585 variable effects along the coast related to the beach characteristics. The spatiotemporal model
586 allows recognizing where storm impact is bigger and where the recovery process is more rapid.

587 Therefore, the spatiotemporal model offers a better understanding of the functioning of the
588 beaches, as well as sometimes recognizing the cause of the sediment imbalances. The methodology
589 offers a rigorous, robust and detailed characterization of the state of the beaches through a large
590 coastal area, making it possible to identify segments of 80 m length too narrow for the maintenance
591 of beach functions as the recreational one. The analysis of these segments in their geographical
592 context allows establishing relations with the morphology of the beaches and their location with
593 respect to artificial structures or natural landforms, offering a diagnosis of the causes of the local
594 lack of sediment. All this information is essential for understanding the dynamics of beaches. It
595 constitutes the first step to adopt solutions to the erosive processes, supporting the coastal planning
596 and the decision-making of the managers.

597 # References

598 Alemany, J. (1984). Estat d'utilització de les platges del litoral català. Barcelona: Departament de Política
599 Territorial i Obres Públiques, Generalitat de Catalunya, Barcelona, 95 pp.

600 Alexandrakis, G., Manasakis, C., & Kampanis, N. A. (2015). Valuating the effects of beach erosion to tourism
601 revenue. A management perspective. Ocean & Coastal Management, 111, 1-11.

602 Almonacid-Caballer, J. (2014). Obtención de líneas de costa con precisión sub-píxel a partir de imágenes
603 Landsat (TM, ETM + y OLI). PhD thesis. Universitat Politècnica de València, Valencia, 365 pp.

Almonacid-Caballer, J. (2015). Extraction of shorelines with sub-pixel precision from Landsat images (TM, ETM+, OLI). Revista de Teledetección, (43), 97-99.

Ballesteros, C., Jiménez, J. A., Valdemoro, H. I., & Bosom, E. (2018). Erosion consequences on beach functions along the Maresme coast (NW Mediterranean, Spain). Natural Hazards, 90(1), 173–195.

Baptista, P., Bastos, L., Bernardes, C., Cunha, T., & Dias, J. (2008). Monitoring sandy shores morphologies by DGPS—a practical tool to generate digital elevation models. Journal of Coastal Research, 24(6), 1516-1528.

Bird, E. C. F. (1996). Beach management (Vol. 5). John Wiley & Son Ltd.

Boak, E. H., & Turner, I. L. (2005). Shoreline definition and detection: a review. Journal of coastal research, 21(4), 688-703.

Bouvier, C., Balouin, Y., & Castelle, B. (2017). Video monitoring of sandbar-shoreline response to an offshore submerged structure at a microtidal beach. Geomorphology, 295, 297-305.

Cabezas-Rabadán, C., Pardo-Pascual, J. E., Palomar-Vázquez, J., Almonacid-Caballer, J., & Fernández-Sarría, A. (2018). La posición de la línea de costa extraída de imágenes satelitales como herramienta de seguimiento y análisis de cambios en playas mediterráneas. XVIII Congreso de Tecnologías de la Información Geográfica, pp. 36-46, 20-22 Jun., València.

Cabezas-Rabadán, C., Rodilla, M., Pardo-Pascual, J. E., & Herrera-Racionero, P. (2019). Assessing users' expectations and perceptions on different beach types and the need for diverse management frameworks along the Western Mediterranean. Land Use Policy, 81, 219–231.

Casella, E., Rovere, A., Pedroncini, A., Stark, C. P., Casella, M., Ferrari, M., & Firpo, M. (2016). Drones as tools for monitoring beach topography changes in the Ligurian Sea (NW Mediterranean). Geo-Marine Letters, 36(2), 151-163.

Castelle, B., Marieu, V., Bujan, S., Splinter, K. D., Robinet, A., Sénéchal, N., & Ferreira, S. (2015). Impact of the winter 2013–2014 series of severe Western Europe storms on a double-barred sandy coast: Beach and dune erosion and megacusp embayments. Geomorphology, 238, 135-148.

Defeo, O., McLachlan, A., Schoeman, D. S., Schlacher, T. A., Dugan, J., Jones, A., … Scapini, F. (2009). Threats to sandy beach ecosystems: A review. Estuarine, Coastal and Shelf Science, *81*(1), 1-12

Do, A. T., de Vries, S., & Stive, M. J. (2018). The Estimation and Evaluation of Shoreline Locations, Shoreline-Change Rates, and Coastal Volume Changes Derived from Landsat Images. Journal of Coastal Research, 35 (1), 56-71.

European Comission. (2009). The Economics of Climate Change Adaptation in EU Coastal Areas. Policy Research Corporation, Spain, 15 pp.

European Commission. (2004). Living with Coastal Erosion in Europe e Sediment and Space for Sustainability. Part I - Major Findings and Policy Recommendations of the EUROSION Project, Office for Official Publications of the European Communities, Luxembourg, 40 pp.

Feagin, R. A., Sherman, D. J., & Grant, W. E. (2005). Coastal erosion, global sea-level rise, and the loss of sand dune plant habitats. Frontiers in Ecology and the Environment, 3(7), 359–364.

Foody, G. M., Muslim, A. M., & Atkinson, P. M. (2005). Super-resolution mapping of the waterline from remotely sensed data. International Journal of Remote Sensing, 26(24), 5381-5392

Gens, R. (2010). Remote sensing of coastlines: detection, extraction and monitoring. International Journal of Remote Sensing, 31(7), 1819-1836.

Ghosh, M. K., Kumar, L., & Roy, C. (2015). Monitoring the coastline change of Hatiya Island in Bangladesh using remote sensing techniques. ISPRS Journal of Photogrammetry and Remote Sensing, 101, 137-144.

GVA (2018). Territorial Action Plan for Green Coastal Infrastructure of the Valencian region (PATIVEL) (2018). Generalitat Valenciana (Spain). Valencian Decree 58/2018. DOGV 11.05.2018

Hagenaars, G., de Vries, S., Luijendijk, A. P., de Boer, W. P. & Reniers, A. J. H. M. (2018). On the accuracy of automated shoreline detection derived from satellite imagery: A case study of the Sand Motor mega-scale nourishment. Coastal Engineering, 133, 113-125

IPCC. (2014). Climate Change 2014: Synthesis Report. Contribution of Working Groups I, II and III to the Fifth Assessment Report of the Intergovernmental Panel on Climate Change. In R. K. Meyer & L. A. Pachauri (Eds.) (p. 151). Geneva, Switzerland.

Jara, M. S., González, M., & Medina, R. (2015). Shoreline evolution model from a dynamic equilibrium beach profile. Coastal Engineering, 99, 1-14.

Jaramillo, C., Sánchez-García, E., Martínez-Sánchez, J., González, M., Medina, R., Palomar-Vázquez, J.M (under review). Calibration and validation of shoreline high-resolution evolution models using remote-sensing techniques. Coastal Engineering.

Jiménez, J. A., Gracia, V., Valdemoro, H. I., Mendoza, E. T. & Sánchez-Arcilla, A (2011). Managing erosion-induced problems in NW Mediterranean urban beaches. Ocean and Coastal Management, 54(12), 907–918. https://doi.org/10.1016/j.ocecoaman.2011.05.003

Jones, B. M., Arp, C. D., Jorgenson, M. T., Hinkel, K. M., Schmutz, J. A., & Flint, P. L. (2009). Increase in the rate and uniformity of coastline erosion in Arctic Alaska. Geophysical Research Letters, 36(3). https://doi.org/10.1029/2008GL036205

Li, J. & Roy, D.P., 2017. A global analysis of Sentinel-2a, Sentinel-2b and Landsat 8 data revisit intervals and implications for terrestrial monitoring. Remote Sensing, 9, 902. https://doi.org/10.3390/rs9090902

Li, W., & Gong, P. (2016). Continuous monitoring of coastline dynamics in western Florida with a 30-year time series of Landsat imagery. Remote Sensing of Environment, 179, 196–209.

Liu, Q., Trinder, J. C., & Turner, I. L. (2017). Automatic super-resolution shoreline change monitoring using Landsat archival data: a case study at Narrabeen–Collaroy Beach, Australia. Journal of Applied Remote Sensing, *11*(1), 016036.

Lubczonek, J. (2017, June). Application of Sentinel-1 imageries for shoreline extraction. In 2017 18th International Radar Symposium (IRS*)* (pp. 1-9). IEEE.

Luijendijk, A., Hagenaars, G., Ranasinghe, R., Baart, F., Donchyts, G., & Aarninkhof, S. (2018). The state of the world's beaches. *Scientific reports*, *8*(1), 6641.

Micallef, A., & Williams, A. T. (2002). Theoretical strategy considerations for beach management. Ocean and Coastal Management, 45(4–5), 261–275. https://doi.org/10.1016/S0964-5691(02)00058-3

Nordstrom KF. (2004). Beaches and dunes of developed coasts. Cambridge, UK: Cambridge University Press

Obiol-Menero, E. M. (2003). La regeneración de playas como factor clave del avance del turismo valenciano. Cuadernos de Geografía. Universidad de Valencia, (73–74), 121–145.

Obiol-Menero, E. M., & Pitarch-Garrido, M. D. (2011). El litoral turístico valenciano. Intereses y controversias en un territorio tensionado por el residencialismo. Boletin de la Asociacion de Geografos Espanoles, (56), 177–200.

Pagán, J. I., Aragonés, L., Tenza-Abril, A. J., & Pallarés, P. (2016). The influence of anthropic actions on the evolution of an urban beach: Case study of Marineta Cassiana beach, Spain. Science of the Total Environment, 559, 242-255.

Pagán, J. I., López, I., Aragonés, L., & Garcia-Barba, J. (2017). The effects of the anthropic actions on the sandy beaches of Guardamar del Segura, Spain. Science of the Total Environment, 601, 1364-1377.

Pajak, M. J., & Leatherman, S. (2002). The high water line as shoreline indicator. Journal of Coastal Research, 18(2), 329-337.

Palomar-Vázquez, J., Almonacid-Caballer, J., Pardo-Pascual, J. E., & Sanchez-García, E. (2018). SHOREX: a new tool for automatic and massive extraction of shorelines from Landsat and Sentinel 2 imagery. 7th International Conference on the Application of Physical Modelling in Coastal and Port Engineering and Science (Coastlab). 22-26 May, Santander.

Palomar-Vázquez, J., Almonacid-Caballer, J., Pardo-Pascual, J. E., Cabezas-Rabadán, C., & Fernández-Sarría, A. (2018). Sistema para la extracción masiva de líneas de costa a partir de imágenes de satélite de resolución media para la monitorización costera: SHOREX. XVIII Congreso de Tecnologías de la Información Geográfica, pp. 36-46, 20-22 Jun., València

Pardo-Pascual, J. E. (1991). La erosión antrópica en el litoral valenciano. Tesis doctorales. Generalitat Valenciana. Conselleria d'Obres Públiques, Urbanisme i Transports.

Pardo-Pascual, J.E. & Sanjaume, E. (2003). Características sedimentológicas y morfológicas de los espacios costeros de transición situados al sur de la desembocadura del Xúquer. Cuadernos de geografía, 73, 183-206.

Pardo-Pascual, J., García-Asenjo, L., Palomar-Vázquez, J., & Garrigues-Talens, P. (2005). New methods and tools to analyze beach-dune system evolution using a Real-Time Kinematic Global Positioning System and Geographic Information Systems. Journal of Coastal Research, Special Issue 49, 34–39.

Pardo-Pascual, J. E., Almonacid-Caballer, J., Ruiz, L. A., & Palomar-Vázquez, J. (2012). Automatic extraction of shorelines from Landsat TM and ETM+ multi-temporal images with subpixel precision. Remote Sensing of Environment, 123, 1–11.

Pardo-Pascual, J. E., Almonacid-Caballer, J., Ruiz, L. A., Palomar-Vázquez, J., & Rodrigo-Alemany, R. (2014). Evaluation of storm impact on sandy beaches of the Gulf of Valencia using Landsat imagery series. Geomorphology, 214, 388-401.

Pardo-Pascual, J., Sánchez-García, E., Almonacid-Caballer, J., Palomar-Vázquez, J., Priego de los Santos, E., Fernández-Sarría, A., & Balaguer-Beser, Á. (2018). Assessing the Accuracy of Automatically Extracted Shorelines on Microtidal Beaches from Landsat 7, Landsat 8 and Sentinel-2 Imagery. Remote Sensing, 10(2), 326.

Pardo-Pascual, J. E., & Sanjaume, E. (2019). Beaches in Valencian Coast. In: Morales J. (eds) The Spanish Coastal Systems (pp 209-236). Springer, Cham

719 Peterson, C.H., Bishop, M.J. (2005). Assessing the environmental impacts of beach nourishment. Bioscience
720 55, 887–896.

721 Psuty, N. P., & Silveira, T. M. (2011). Tracking Coastal Geomorphological Change: an application of protocols
722 to collect geotemporal data sets at the national level in the US. Journal of Coastal Research, Special Issue 64,
723 1253-1257.

724 Pye, K., & Blott, S. J. (2016). Assessment of beach and dune erosion and accretion using LiDAR: impact of the
725 stormy 2013–14 winter and longer term trends on the Sefton Coast, UK. Geomorphology, 266, 146-167.

726 Ranasinghe, R., Holman, R., de Schipper, M., Lippmann, T., Wehof, J., Duong, T. M., ... & Stive, M. (2012).
727 Quantifying nearshore morphological recovery time scales using argus video imaging: Palm Beach, Sydney and
728 Duck, North Carolina. *Coastal Engineering Proceedings*, *1*(33), 24.

729 Rico-Amoros, A. M., Olcina-Cantos, J., & Saurí, D. (2009). Tourist land use patterns and water demand:
730 Evidence from the Western Mediterranean. Land Use Policy, 26(2), 493-501.

731 Saleem, A., & Awange, J. L. (2019). Coastline shift analysis in data deficient regions: Exploiting the high spatio-
732 temporal resolution Sentinel-2 products. *CATENA*, *179*, 6-19.

733 Sánchez-García, E., Palomar-Vázquez, J.M., Pardo-Pascual, J.E., Almonacid-Caballer, J., Cabezas-Rabadán, C.,
734 Gómez-Pujol, L. (under review). An efficient protocol for accurate and massive shoreline definition from mid-
735 resolution satellite imagery. Coastal Engineering.

736 Sánchez-García, E., Balaguer-Beser, A., & Pardo-Pascual, J. E. (2017). C-Pro: A coastal projector monitoring
737 system using terrestrial photogrammetry with a geometric horizon constraint. ISPRS Journal of
738 Photogrammetry and Remote Sensing, 128, 255-273. https://doi.org/10.1016/j.isprsjprs.2017.03.023

739 Sanjaume, E. (1985). Las costas valencianas: sedimentología y morfología. PhD Thesis. Universitat de València,
740 València, 505 pp.

741 Sanjaume, E., & Pardo-Pascual, J. E. (2005). Erosion by human impact on the Valencian coastline (E of Spain).
742 Journal of Coastal Research, Special Issue 49, 76–82.

743 Sanjaume, E., & Pardo-Pascual, J. E. (2007). Cambios de tendencias recientes en la evolución costera del golfo
744 de Valencia: análisis espaciales y sedimentológicos. Actas de las Jornadas Técnicas Las nuevas técnicas de
745 información geográfica al servicio de la gestión de zonas costeras: Análisis de la evolución de playas y dunas,
746 5–11.

747 Sanjaume, E., Pardo-Pascual, J. E., & Segura-Beltran, F. (2019). Mediterranean Coastal Lagoons. In: Morales J.
748 (eds) The Spanish Coastal Systems (pp 237-267). Springer, Cham.

749 Sardá, R., Mora, J., Ariza, E., Avila, C., & Jimenez, J. A. (2009). Decadal shifts in beach user sand availability on
750 the Costa Brava (Northwestern Mediterranean Coast). Tourism Management, 30(2), 158–168.
751 https://doi.org/10.1016/j.tourman.2008.05.011

752 Schlacher, T. A., Schoeman, D. S., Dugan, J., Lastra, M., Jones, A., Scapini, F., & McLachlan, A. (2008). Sandy
753 beach ecosystems: key features, sampling issues, management challenges and climate change impacts.
754 Marine ecology, 29, 70-90.

755 Segura-Beltran F., Pardo-Pascual J.E. (2019). Fan Deltas and Floodplains in Valencian Coastal Plains. In:
756 Morales J. (eds) The Spanish Coastal Systems (pp. 489-516). Springer, Cham

Song, J., Fu, X., Wang, R., Peng, Z. R., & Gu, Z. (2018). Does planned retreat matter? Investigating land use change under the impacts of flooding induced by sea level rise. Mitigation and Adaptation Strategies for Global Change, 23(5), 703-733.

Speybroeck, J., Bonte, D., Courtens, W., Gheskiere, T., Grootaert, P., Maelfait, J.P., Mathys, M., Provoost, S., Sabbe, K., Stienen, E.W.M., Van Lancker, V., Vincx, M., Degraer, S. (2006). Beach nourishment: An ecologically sound coastal defence alternative? A review. Aquat. Conserv. Mar. Freshw. Ecosyst. 16(4), 419–435.

Stive, M. J., Nicholls, R. J., & DeVriend, H. J. (1991). Sea-level rise and shore nourishment: a discussion. Coastal Engineering, 16, 147-163.

Stronkhorst, J., Huisman, B., Giardino, A., Santinelli, G. and Duarte Santos, F. (2018): Sand nourishment strategies to mitigate coastal erosion and sea level rise at the coast of Holland (The Netherlands) and Aveiro (Portugal) in the 21st century, Ocean & Coastal Management, 156, 266-276.

Tsai, V. J. (1993). Delaunay triangulations in TIN creation: an overview and a linear-time algorithm. International Journal of Geographical Information Science, 7(6), 501-524.

Turner, I. L., Harley, M. D., & Drummond, C. D. (2016). UAVs for coastal surveying. Coastal Engineering, 114, 19-24.

Vandebroek, E., Lindenbergh, R., van Leijen, F., de Schipper, M., de Vries, S. and Hanssen, R. (2017). Semi-automated monitoring of a mega-scale beach nourishment using hig-resolution TerraSAR-X satellite data, Remote Sensing, 9, 633.

Williams, A. T., Rangel-Buitrago, N., Pranzini, E., & Anfuso, G. (2018). The management of coastal erosion. Ocean & Coastal Management, 156, 4-20.

Yates, M.L., Guza, R.T., O'Reilly, W.C. (2009). Equilibrium shoreline response: Observations and modeling. Journal of Geophysical Research: Oceans, 114 (C09014): 1-16.

Yepes, V. (2002). Ordenación y gestión del territorio turístico. Las playas. (D. Blanquer, Ed.). Valencia: Tirant lo Blanch.

Yepes, V., & Medina, J. R. (2005). Land Use Tourism Models in Spanish Coastal Areas. A Case Study of the Valencia Region. Journal of Coastal Research, (49), 83–88.

A dataset of Satellite-Derived Shorelines (SDS) is available at http://cgat.webs.upv.es/datasets/